Evaluations of CTOD and J-integral for Three-point Bend Specimens with Shallow Cracks

SHANG-XIAN WU

Department of Mechanical Engineering, University of Sydney, NSW 2006, Australia

ABSTRACT

Analytical predictions and experimental determinations of near–field and far–field plastic rotation factors and J–integral estimation formula for three–point specimens with deep and shallow cracks are presented. Tests of CTOD and J–integral carried out for a free–cutting steel show that the initiation fracture toughness (δ_i and J_{IC}) are higher for shallow cracks than for deep cracks by a factor of approximately 2.3 and 2.7 respectively.

KEYWORDS

Elastic–plastic fracture test, shallow crack, rotation factor, crack tip opening displacement, J–integral

INTRODUCTION

Most standard elastic–plastic fracture toughness test methods recommend the use of deeply–cracked specimens. Fracture toughness data are therefore mainly obtained on such specimens. However, in structures, particularly welded ones, many defects are in the form of shallow cracks. Recent results (Chipperfield, 1978; Cotterell *et al.*, 1985; Matsoukas, *et al.*, 1986a, Thompson and Knott, 1986; Towers and Garwood, 1986) show that the elastic–plastic fracture toughness values at initiation of crack growth (δ_i or J_{IC}) are higher for shallow cracks than for deep cracks. Consequently the assessment of the significance of a practical shallow defect using a value of fracture toughness from a standard test with deeply–cracked specimens can be unduly conservative. There is increasing interest in fracture toughness tests of shallow crack specimens with the aim of better understanding the behaviour of shallow cracks. The purpose of this paper is to discuss the crack tip opening displacement (CTOD) and J–integral test methods of three–point bend specimens with shallow cracks.

CALCULATIONS OF CTOD AND J–INTEGRAL

Plastic Rotation Factors (r_p)

In standard methods the crack tip opening displacement (CTOD), δ, is obtained from the sum of elastic component (δ_e) and plastic component (δ_p). δ_e is calculated from the nominal stress–intensity factor K induced by the applied load and δ_p is calculated from the plastic component of the crack mouth opening displacement V_p according to the plastic hinge model, which assumes that two rigid arms of the specimen rotate about a plastic hinge point in the uncracked ligament. The distance of the plastic hinge point from the crack tip is $r_p(W-a)$, where W is the specimen width, a is the crack length and r_p is the plastic rotation factor. A problem of CTOD test of shallow crack specimens is the determination of the plastic rotation factor r_p. There are two definitions of r_p: the far–field and the near–field definitions. The far–field plastic rotation factor r_{fp} is defined by use of displacements far from the crack tip such as the crack mouth opening displacement V_p and the load–point displacement q_p according to the plastic hinge deformation model. The plastic rotation factor determined by the use of the double clip–gauge method (Lin *et al.*, 1982; Matsoukas *et al.*, 1984; Towers and Garwood, 1986; Wu, 1983) is r_{fp}. The near–field plastic rotation factor r_{np} is calculated from the V_p and the near–field measurement of δ_p obtained from, a replica, a section or the stretched zone width (SZW) by assuming in each case that the crack surfaces to remain straight. Hence

$$r_{np} = \frac{a + z}{W - a}\frac{\delta_p}{V_p - \delta_p} \tag{1}$$

where z is the thickness of the knife–edges. The slip–line field in Fig. 1 shows that the deformation of a deeply–cracked three point bend specimen follows the plastic hinge model. The theoretical values of r_{fp} predicted by the slip–line field and finite element analyses are in agreement (Wu *et al.*, 1988b) with each other. These also agree with the experimental values of r_{fp} and r_{np} (Lin *et al.*, 1982; Matsoukas *et al.*, 1984; Wu, 1983). For specimens with shallow cracks ($a/W \leq 0.172$) the slip–line field analyses (Wu *et al.*, 1988a) show that the crack face and the crack mouth are within the rigid zone KGCVT (Fig. 2), which rotates about the uncracked ligament with angular velocity ω_2. The specimen arms rotate with angular velocity ω_1. The slip–line field solutions give

$$\frac{\omega_1}{\omega_2} = 1.747 - 6.829\frac{a}{W} + 14.74\left[\frac{a}{W}\right]^2, \qquad \text{for } \frac{a}{W} \leq 0.172 \tag{2}$$

For $a/W > 0.172$, $\omega_1/\omega_2 = 1$. If the plastic deformation is small as in the case of the CTOD test, the deformation geometry gives

$$r_{fp} = \frac{W}{W - a}\frac{\omega_1}{\omega_2}\frac{V_p}{q_p} - \frac{a + z}{W - a} \tag{3}$$

Fig. 3 shows the r_{fp} values predicted by slip–line field analyses for perfectly plastic materials (solid line) and by use of the finite element data of Kumar *et al.* (1981) for power–law hardening materials (n=2 to 20). Since the deformation of crack tip involves blunting and finite strain, there is no available analytical result of r_{np}. The experimental methods for the determination of r_{fp} and r_{np} are described below.

J–integral Estimation Formula

In ASTM E813 J–integral is estimated by

$$J = J_e + J_p = \frac{K^2}{E'} + \frac{\eta_p A_p}{B(W-a)} \tag{4}$$

where A_p is the plastic part of the area under the load vs load–point displacement curve. η_p, the plastic η–factor, is taken as 2 for deeply cracked three–point bend specimens in ASTM E813. For shallow crack specimens η_p can be derived from the limit load P_L of the specimen according to

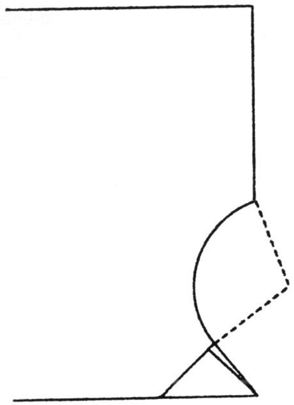

Fig. 1 Slip-line field of three-point bend specimen with deep crack.

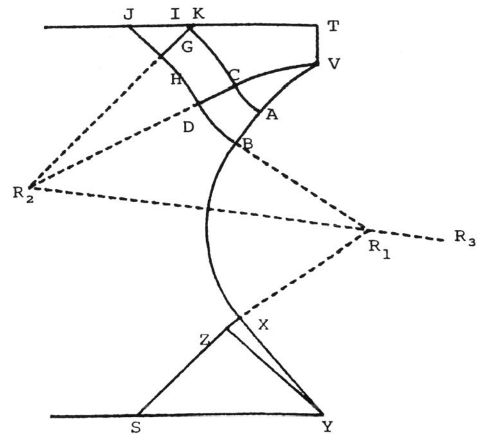

Fig. 2 Slip-line field of three-point bend specimen with shallow crack.

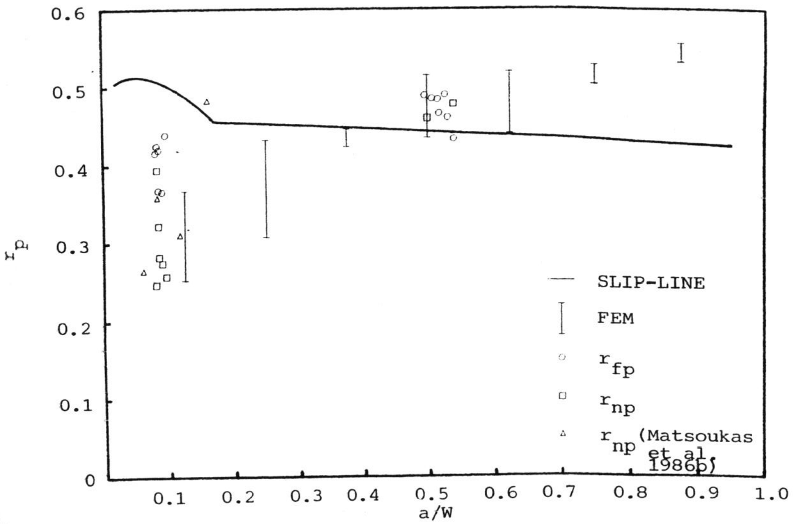

Fig. 3 Comparisons of analytical predictions of r_{fp} and experimental results of r_{fp} and r_{np}.

$$\eta_P = -\left(1-\frac{a}{W}\right)\frac{1}{P_L}\frac{\partial P_L}{\partial(a/W)}\,. \qquad (5)$$

Towers and Garwood (1986) and Sumpter (1987) used η_P–factor obtained from the limit load of pure bending specimens to J_{IC} tests of three point bend specimens. This procedure is clearly incorrect. It is possible to obtain theoretical slip–line field solutions of three point bend specimens which give

$$P_L = \left[1.125 + 0.892\,\frac{a}{W} - 2.238\left(\frac{a}{W}\right)^2\right]\frac{2}{\sqrt{3}}\,\frac{(W-a)^2}{S}\,B\,\sigma_{ys}, \qquad (6)$$

for $\frac{a}{W} \leq 0.172$. S is the span, B is the specimen thickness and σ_{ys} is the yield strength of the material. Hence

$$\eta_P = 2 - \frac{(1-a/W)(0.892-4.476\,a/W)}{1.125 + 0.892\,a/W - 2.238\,(a/W)^2}\,, \qquad (7)$$

for $a/W \leq 0.172$.

MATERIALS AND EXPERIMENTAL PROCEDURES

The test material was a free–cutting steel in normalized condition with the composition: 0.060 C, 1.16 Mn, 0.29 S, 0.075 Si, 0.066 P, 0.018 Ni, 0.012 Cr, 0.002 Mo, 0.016 Cu, 0.002 V and 0.002 N. The mechanical properties were: yield strength σ_{ys} = 202 MPa, ultimate tensile strength σ_{ts} = 338 MPa, elongation = 29.3% and reduction of area = 34.9%. Specimens of B = 14 mm, W = 25 mm were machined so that the length and width dimensions lay in a plane normal to the rolling direction. The elongated MnS inclusions were therefore parallel to the crack front. Two crack length ratios a/W = 0.5 and a/W = 0.1 were used. The low a/W ratio was obtained by fatigue–precracking the specimens and then reducing the width to W = 22.5 mm to produce the desired a/W ratio. A pair of integrated knife–edges for mounting clip–gauge were machined on each shallow crack specimen. The distance between the knife–edges was 5 mm and the knife–edges were within the rigid zones.

Tests were performed in three–point bending using an Instron 1195 testing machine at a constant displacement rate of 0.1 mm/min. Two clip gauges were used, one for crack mouth opening displacement (V), another for load–point displacement (q). For each specimen P–V and q–V records were taken on an X–Y–Y chart recorder and P–q record was taken on a second X–Y recorder. Individual specimens were unloaded from different positions along the P–V curves to obtain different amount of crack growth Δa. All unloaded shallow crack specimens and two unloaded deeply–cracked specimens were sectioned at distances of 1/6, 1/3 and 1/2 thickness from one free surface of the specimen. The sections of shallow crack specimens were polished and etched. Near–field measurements of δ_P at the original crack tip were made on the three sections and an average was obtained for each specimen. The sections of deeply–cracked specimen were aged at 250°C for 30 minutes and then were polished and etched using Fry's reagent to reveal the plastic deformation bands. A mark was made at the upper boundaries of the deformation bands as shown in Fig. 6. Then the sections were repolished and near–field measurements of δ_P were made at the mark. The remained unsectioned parts of the specimens were heat–tinted and then were broken open at liquid nitrogen temperature. Other unloaded deeply–cracked specimens were directly heat–tinted and broken open at the temperature of liquid nitrogen. Crack length and crack extension were measured from the broken surfaces and the sections.

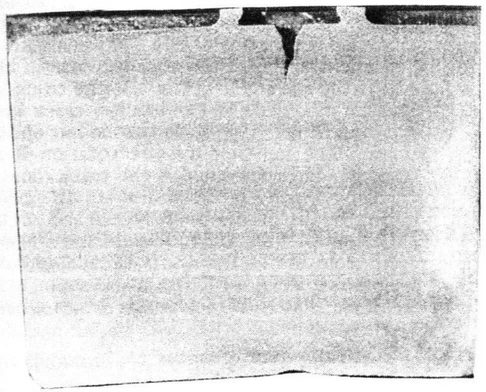

Fig. 4. Fry's etched section of shallow crack specimen.

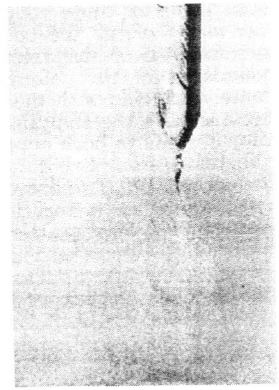

Fig. 5. Fry's eched section of deep crack specimen.

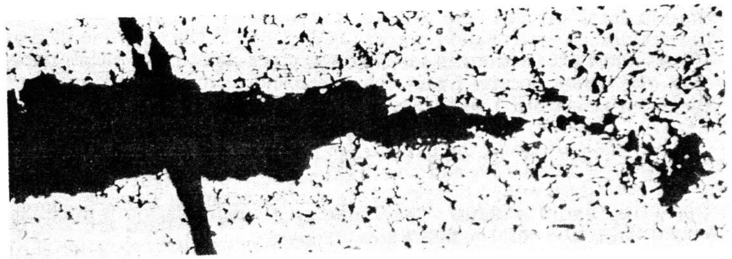

Fig. 6. Micrograph of crack tip of deep crack specimen showing the crack tip and the mark.

RESULTS AND DISCUSSION

Plastic rotation factors

Values of r_{fP} were calculated using Eq. (3). The (V_P/q_P) ratios were taken as the slopes of the V–q records after general yielding of the specimen. The experimental records show that after general yielding increases in load P were small and the V–q records were straightlines. Therefore the slopes of the V–q lines represent the ratio of ΔV_P and Δq_P. The experimental results of r_{fP} are also given in Fig. 3 alongside the theoretical predictions. Values of r_{nP} were calculated using Eq. (1) with the near–field measurements of δ_P made on the sections. The results of r_{nP} and those obtained previously by Matsoukas et al. [1986b] are also represented in Fig. 3.

It can be seen that for deeply–cracked specimens the predictions of r_{fp} given by slip–line field and finite element analyses and the experimental values of r_{fp} and r_{np} are in good agreement. In practical specimens the idealized isolated slip–lines in Fig. 1 become deformation bands of finite width. Observations show that the width of deformation bands increases towards the bottom free surface of the specimen as the deformation increases. Because of the unidirectional thickening towards the bottom surface the upper boundaries of the deformation bands, i.e. the boundaries of the rigid zones, approximately coincide with the tip of the precrack. Therefore r_{fp} and r_{np} agree with each other and with the analytical predictions. For shallow crack specimens the plastic deformation spreads to both upper and bottom surfaces. Thickening of the deformation bands is therefore along two directions (i.e. towards both upper and lower surfaces) and the rigid zone KGCVT is reduced. This makes accurate measurements of V_p extremely difficult and consequently makes the calculations of r_{fp} and r_{np} using Eqs. (1) and (3) highly suspect. The large scatter of r_p shown in Fig. 3 supports this conclusion. There is also some discrepancy between the r_{fp} predictions given by the slip–line field and finite element analyses. Similar experimental results of r_{fp} are obtained by Sumpter (1987) who did not take account for the factor $\omega 1/\omega_2$. You (1984) gave the experimental values of r_{np} = 0.2 and 0.15 for four–point bend specimens with a/W = 0.2 and 0.1 respectively. But the equation for calculation of r_{np} used by You

$$r_{np} = \frac{a+z}{W-a}\frac{V_p}{\delta_p} \quad (8)$$

is incorrect. With the correct equation (1) much higher r_{np} values would have been obtained from You's data. All these problems point to the difficulty of using the plastic rotation concept to evaluate CTOD in shallow crack specimens.

CTOD Test

P–V records and etched sections show that fibrous crack growths for both deep and shallow crack specimens occurred after general yielding. Values of δ for deep cracks were calculated using the BS 5762 procedures except with r_p = 0.45 as suggested in our earlier work. For shallow cracks δ_p were measured from three cut sections across the thickness. δ_e were calculated in the usual way and added to δ_p to give the total δ. Fig. 4 shows the data of δ versus Δa and the linear regression δ–R curves. Values of δ_i at crack initiation were determined by the points of intersection of the δ–R curves and the theoretical blunting line $\delta = 2\Delta a$. The values of δ_i thus obtained are δ_i(a/W = 0.5) = 0.082 mm and δ_i(a/W = 0.1) = 0.192 mm. Therefore, for the test material, the effect of reducing a/W from 0.5 to 0.1 is to increase δ_i by a factor of 2.3. This effect is related to the reduction of stress–triaxility ahead of the shallow crack tip due to the plastic deformation spreading to both specimen surfaces. The slip–line field analyses show that the maximum hydrostatic stress ahead of the crack tip reduces from 3.35 k for a/W = 0.5 to 2.37 k for a/W = 0.1, where k is the shear yield stress of the material.

J–integral Test

Values of J–integral for deeply–cracked specimens were calculated using ASTM E813 procedures. Values of J for shallow crack specimens were calculated using Eqs. (4) and (7) but were qualified using ASTM–E813 procedures. The J–Δa data and the linear regression J–R curves are plotted in Fig. 5. The J_{IC} values were determined from the points of intersection of the J–R curves and the blunting line $J = 2\sigma_y \Delta a$, where σ_y is the average of σ_{ys} and σ_{ts}. The test results show that J_{IC} increases from 30.3 kJm^{-2} for a/W = 0.5 to 81.0 kJm^{-2} for a/W = 0.1 by a factor of 2.7.

It seems that the shallow crack data in Fig. 8, if fitted to a curve, might agree with the deep crack data. However, it should be noted that the inclusion of the rejected data

point (Δa = 0.18 mm, J = 58.8 kJm^{-2}) just outside the 0.15 mm exclusion line into J–R curve regression would give J_{IC} = 64.0 kJ m^{-2} for the shallow crack. On the other hand, the interpretation of the qualified data in terms of the procedure of power curve fitting and 0.2 mm offset line give J_{IC}(a/W = 0.5) = 44.6 kJ m^{-2} and J_{IC}(a/W = 0.1) = 76.9 kJ m^{-2} respectively. Therefore, it can be concluded that the effect of a/W is not due to the uncertainty of interpretation.

CONCLUSIONS

Analytical predictions and methods for experimental determination of near–field and far–field plastic rotation factors of three–point bend specimens are presented. The experimental results for a free–cutting steel show that r_{np} and r_{fp} are the same for deeply–cracked specimens, but are difficult to measure accurately for shallow crack specimens. The effects of reducing crack length from a/W = 0.5 to a/W = 0.1 on the test material are that the fracture toughness at initiation of crack growth in terms of δ_i and J_{IC} increases by a factor 2.3 and 2.7 respectively. These effects are related to the reduction of the stress–triaxility ahead the crack tip as the crack length is reduced.

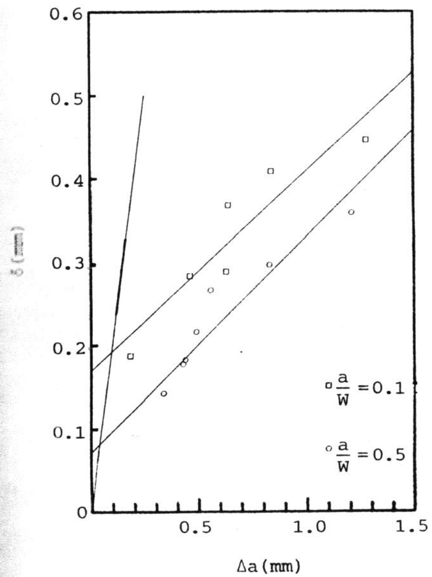

Fig. 7 δ-R curves for deep and shallow crack specimens.

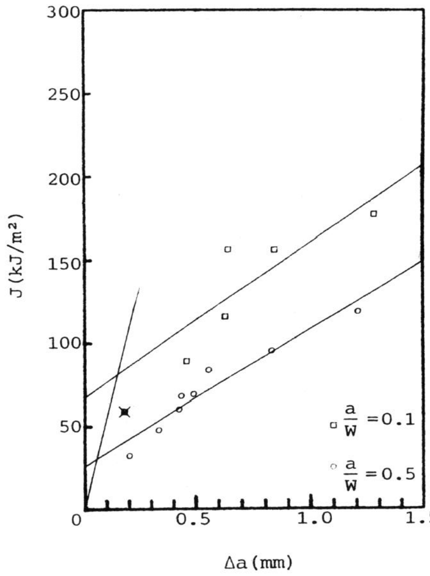

Fig. 8 J-R curves for deep and shallow crack specimens. ✕ represents the rejected data.

Acknowledgement

I wish to thank the University of Sydney for a Postgraduate Research Award and the Australian Welding Research Association for the Sir William Hudson Memorial Award. I wish also to thank Professor Y–W. Mai and Dr. B. Cotterell for useful discussion on this work.

REFERENCES

ASTM E813–83. Standard test for J_{Ic}, a measure of fracture toughness.

BS 5762 (1979). British Standard, Method for crack opening displacement (COD) testing.

Chipperfield, C.G. (1978). Some observations on ductile crack initiation and propagation in fracture toughness specimens. Proc. Specialists Meeting on Elastic–Plastic Fracture Mechanics, Vol. 2, OECD Nuclear Energy Agency Daresburg, Paper 15.

Cotterell, B., Q.–F. Li, D.–Z. Zhang and Y.–W. Mai (1985). On the effect of plastic constraint on ductile tearing in a structural steel. Engng Fract. Mech., 21, 239–244.

Lin, I.H., T.L. Anderson, R. De Witt and M.G. Dawes (1982). Displacements and rotational factors in single edge notched bend specimens. Int. J. Fracture, 20, R1–7.

Kumar, V., M.D. German and C.F. Shih (1981). An engineering aproach for elastic–plastic fracture analysis, Topical Report No. EPRI–NP–1931, Research Project 1237–1, General Electric Company, Schenectady, N.Y.

Matsoukas, G., B. Cotterell and Y.–W. Mai, (1984). On the plastic rotation constant used in standard COD tests. Int. J. Fracture, 26, R49–53.

Matsoukas, G., B. Cotterell and Y.–W. Mai (1986a). The effect of shallow cracks on crack tip opening displacement. Engng. Fract. Mech., 24, 837–842.

Matsoukas, G., B. Cotterell and Y–W. Mai (1986b). Hydrostatic stress and crack opening displacement in three–point bend specimens with shallow cracks. J. Mech. Phys. Solids, 34, 499–510.

Sumpter, J.D.G. (1987). J_c determination for shallow notch welded bend specimens. Fatigue Fract. Engng. Mater. Struct., 10, 479–493.

Thompson, H.E. and J.F. Knott, (1986). Effects of crack length and prestrain on ductile fracture. Fracture Control of Engineering Structures, ECF–6.

Towers, O.L. and S.J. Garwood (1986). Influence of crack depth on resistance curves for three–point bend specimens in HY130. Fracture Mechanics: Seventeenth Volume, ASTM STP 905, 454–484.

Wu, S.–X. (1983). Plastic rotational factor and J–COD relationship of three–point bend specimen. Engng Fract. Mech., 18, 83–95.

Wu, S.–X., B. Cotterell and Y.–W. Mai (1988a). Slip–line field solutions for three–point notched–bend specimens. Int. J. Fracture, (in press).

Wu, S.–X., Y.–W. Mai and B. Cotterell (1988b). Plastic rotation factors of three–point bend and compact tension specimens. Journal of Testing and Evaluation, (in press).

You, C.P. (1984). Mechanisms of fracture in high strength steels. PhD Thesis, University of Cambridge.